Neuropsychologia 161 (2021) 108011

Contents lists available at ScienceDirect

Neuropsychologia

journal homepage: www.elsevier.com/locate/neuropsychologia

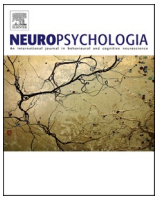

Visual search performance in cerebral visual impairment is associated with altered alpha band oscillations

Christopher R. Bennett [a], Corinna M. Bauer [a], Peter J. Bex [b], Davide Bottari [c,1], Lotfi B. Merabet [a,*,1]

[a] The Laboratory for Visual Neuroplasticity, Department of Ophthalmology, Massachusetts Eye and Ear, Harvard Medical School, Boston, MA, USA
[b] Translational Vision Lab, Department of Psychology, Northeastern University, Boston, MA, USA
[c] IMT School for Advanced Studies, Lucca, Italy

A B S T R A C T

Individuals with cerebral visual impairment (CVI) often present with deficits related to visuospatial processing. However, the neurophysiological basis underlying these higher order perceptual dysfunctions have not been clearly identified. We assessed visual search performance using a novel virtual reality based task paired with eye tracking to simulate the exploration of a naturalistic scene (a virtual toy box). This was combined with electroencephalography (EEG) recordings and an analysis pipeline focusing on time frequency decomposition of alpha oscillatory activity. We found that individuals with CVI showed an overall impairment in visual search performance (as indexed by decreased success rate, as well as increased reaction time, visual search area, and gaze error) compared to controls with neurotypical development. Analysis of captured EEG activity following stimulus onset revealed that in the CVI group, there was a distinct lack of strong and well defined posterior alpha desynchronization; an important signal involved in the coordination of neural activity related to visual processing. Finally, an exploratory analysis revealed that in CVI, the magnitude of alpha desynchronization was associated with impaired visual search performance as well as decreased volume of specific thalamic nuclei implicated in visual processing. These results suggest that impairments in visuospatial processing related to visual search in CVI are associated with alterations in alpha band oscillations as well as early neurological injury at the level of visual thalamic nuclei.

1. Introduction

Cerebral (or cortical) visual impairment (CVI) is the leading individual cause of pediatric visual impairment in developed countries (Solebo et al., 2017). It represents a brain based visual condition and has been defined as verifiable visual dysfunction associated with damage to retrochiasmatic pathways and cerebral structures (Dutton, 2003; Sakki et al., 2018). The most common cause of CVI is perinatal hypoxic-ischemic injury (associated with periventricular leukomalacia and hypoxic-ischemic encephalopathy), and other common causes include head injury/trauma, infection, as well as genetic and metabolic disorders (Hoyt, 2003). This early neurological injury is believed to dramatically alter the development of brain areas including cortical gray matter, white matter tracts, and subcortical structures (Volpe, 2009). Despite the fact that CVI represents a significant global public health concern, the neurophysiological basis of visual impairments and their association with early neurological injury have not yet been clearly identified.

The range of visual deficits in CVI include possible decreased visual acuity and visual field restriction. Interestingly, even when these measures of visual function are within normal range, many individuals with CVI also present with impairments related to higher order visuospatial processing and attention (Fazzi et al., 2007; Philip and Dutton, 2014; Zihl et al., 2015). Often these individuals exhibit difficulties carrying out visual tasks in crowded and cluttered environments as well as in dynamic visual scenes with complex moving objects (Lam et al., 2010; McDowell and Dutton, 2019). As a simple example, a child with CVI may recognize a favorite toy when presented in isolation, but have difficulty finding it when placed in a box filled with other toys. These visual perceptual dysfunctions can have a negative impact on overall functioning and independence (McKillop and Dutton, 2008; Boot et al., 2010; Dutton, 2013). Furthermore, given the heterogeneous profile of CVI (with respect to clinical presentation and underlying cause), making an accurate diagnosis can be very challenging. Typically, higher order visual processing deficits are not assessed as part of a standard ophthalmological exam (Williams et al., 2011; van Genderen et al.,

* Corresponding author. Department of Ophthalmology, Massachusetts Eye and Ear Infirmary, Harvard Medical School, 20 Staniford Street, Boston, MA, 02114, USA.
E-mail address: lotfi_merabet@meei.harvard.edu (L.B. Merabet).
[1] Equal contributing senior authors.

https://doi.org/10.1016/j.neuropsychologia.2021.108011
Received 29 April 2021; Received in revised form 30 July 2021; Accepted 26 August 2021
Available online 30 August 2021

2012) and basing diagnosis on simple criteria such as visual acuity alone fails to capture the complex spectrum of visual perceptual difficulties seen in this population (Martin et al., 2016). Thus, an improved characterization of visual processing deficits beyond standard measures of visual function (along with a better understanding of their neurophysiological basis) can not only help enhance diagnosis, but also guide the development of appropriate and individualized compensatory strategies in this population (for further discussion, see (McDowell, 2020)).

In the clinical setting, electrophysiological testing such as visual evoked potential (VEP) recordings have been used to characterize the integrity and function of anterior (afferent) visual pathways. VEP testing in CVI can be a useful method to estimate visual acuity function, particularly in the case of younger patients who cannot undergo formal testing ((Skoczenski and Norcia, 1999, Good et al., 2001; Watson et al., 2010), see (Chang and Borchert, 2020) for review, but also (Lim et al., 2005) regarding disparities with different evaluation methods and limitations). However, there are important limitations associated with traditional VEP testing, particularly in the context of uncovering the neurophysiological basis of higher order visual processing deficits in CVI. These are related to the nature of the visual stimuli and tasks employed, as well as interpretations drawn from the analysis of acquired signals. The VEP is typically recorded in response to simple visual stimuli such as flashing lights or patterns like gratings or checkerboards. As such, these stimuli are not likely to fully capture subtle deficits related to higher order visual processing when viewing more complex and naturalistic scenes. As mentioned previously, this issue is of critical importance as there is often a mismatch between measures of visual function (such as visual acuity) and how an individual with CVI functions in real world situations (Williams et al., 2011). Thus, on a first level, there is a need to develop novel assessment methods to characterize functional visual abilities in settings that more closely approximate real-world, naturalistic scenes as well as incorporate tasks that have high behavioral and functional relevance (Bennett et al., 2019). For this purpose, virtual reality (VR) has numerous advantages in assessing behavioral performance including task realism, adaptability, and experimental control, while maintaining objective data capture and participant engagement (Parsons, 2015; Bennett et al., 2019). With respect to characterizing visuospatial processing abilities, a VR-based simulation can also be combined with a visual search paradigm. Visual search assesses an individual's ability to find a target hidden amongst a field of distractors and thus, can serve as an important proxy regarding the spatial processing of visual information and the deployment of attention (Treisman and Gelade, 1980).

It is also important to note that while VEP recordings can be used to evaluate the function of anterior visual pathways and estimate measures of visual function (e.g. visual acuity), their potential utility is less clear in the setting of lesions occurring posterior to the optic chiasm or beyond primary visual cortex (such as in the case of CVI). For example, the VEP waveform may be normal in patients with cortical blindness, despite evidence of extensive bi-occipital damage ((Fera et al., 1990)) see also (Aminoff, 2007)). Accordingly, there is also a need for more advanced electroencephalogram (EEG) based analyses that can provide insight as to how information is encoded, transferred, and integrated between distinct brain regions across multiple temporal scales (Siegel et al., 2012). The human EEG is characterized by several prominent and important frequency band signals. Notably, posterior alpha oscillatory activity (within the 8–12 Hz band) reflects excitatory/inhibitory balance within the visual system (Jensen et al., 2012; Klimesch, 2012; Clayton et al., 2018). Alpha synchronization (i.e. an increase in alpha activity) results in an inhibition of task-irrelevant neural circuits, while alpha desynchronization (i.e. a decrease in alpha activity) results from the engagement of task relevant neural processing (Jensen et al., 2012; Klimesch, 2012). The role of alpha oscillatory activity with regard to visual perception and spatial attention in humans has been supported by electro- and magnetoencephalography studies showing reduced alpha oscillatory amplitude in response to perceived visual stimuli and attention orientating (Thut et al., 2006; Capilla et al., 2014). In this direction, the analysis of alpha oscillations in CVI could be helpful in characterizing electrophysiological signals associated with visual search performance.

In this study, we attempted to address these issues for the purposes of characterizing visuospatial processing deficits in CVI and uncovering their neurophysiological basis. Specifically, we developed a combined behavioral-EEG paradigm to assess visual search performance using eye tracking with a novel, behaviorally relevant VR-based task simulating a naturalistic scene (specifically, searching for a toy in a toy box). This was combined with EEG recordings, with a particular focus on analyzing alpha oscillatory activity in relation to visual search performance. From a behavioral standpoint (and consistent with previous reports of visuospatial processing deficits in this population), we hypothesized that individuals with CVI would show an impairment in visual search performance compared to controls with neurotypical development. We further surmised that impaired visual search would be associated with alterations in oscillatory activity following stimulus onset. Specifically, we expected altered alpha desynchronization responses over occipital areas compared to controls. This finding would be consistent with current evidence that oscillatory activity in this frequency band is implicated with the coordination of neural activity related to perceptual and cognitive tasks (including attention orienting), and also represents an important marker of functional brain development. Finally, we explored putative associations between the amplitude of alpha oscillations and measures of visual function (i.e. visual acuity), behavioral performance related to our visual search task, and structural morphometry at the level of visual thalamic nuclei.

2. Methods

2.1. Participants

A total of 22 individuals participated in the study. Of these, ten were clinically diagnosed with CVI and aged between 15 and 22 years (3 female, mean age: 17.5 years old ± 2.59 SD). All had visual impairments related to perinatal neurological injury including hypoxic/ischemic damage, periventricular leukomalacia (PVL) associated with prematurity, or other causes (e.g. infection, genetic). Four out of the ten participants were born preterm (i.e. prior to 37 weeks gestation). Best corrected visual acuity ranged from 20/20 to 20/60 (Snellen equivalent; in the better seeing eye). All had ocular motor fixation sufficient to perform the behavioral task and intact visual field function within the area corresponding to the visual stimulus presentation (a full list of participant details can be found in Table 1). Twelve individuals with neurotypical development and aged between 14 and 25 years (5 female, mean age: 19.92 years old ± 2.61 SD) served as comparative controls. Control participants had normal or corrected to normal visual acuity and no previous history of any ophthalmic (e.g. strabismus, amblyopia) or neurodevelopmental (e.g. epilepsy, attention deficit disorder) conditions. The groups were not statistically different with respect to mean age ($p = 0.1204$). All components of the study were approved by the investigative review board of the Massachusetts Eye and Ear, Boston MA, USA and consent was obtained from all the participants and a parent/legal guardian (in the case of a minor) prior to commencing the study. The study was approved by the Investigative Review Board at the Massachusetts Eye and Ear in Boston, MA, USA and carried out in accordance to the Code of Ethics of the World Medical Association (Declaration of Helsinki) for experiments involving humans.

2.2. Behavioral task and visual stimulus design

We developed a desktop VR-based visual search task referred to as the "virtual toy box" (complete details regarding the design of the task can be found in (Bennett et al., 2018)). Briefly, the behavioral task represents a simulated rendering of a toy box with a 5 × 5 array of static

Table 1
CVI participant demographics.

Subject ID	Sex	Age	Associated Cause of CVI	Preterm (<37 weeks)/ term	Distance Visual Acuity OD - OS (Snellen)	Distance Visual Acuity OD - OS (LogMAR equivalent)
1	female	15	birth complication, global developmental delay	Term	20/30–20/30	0.2–0.2
2	female	17	meningitis, infarct	Term	20/50–20/60	0.4–0.5
3	male	19	decreased placental perfusion	preterm	20/25–20/25	0.1–0.1
4	female	21	periventricular leukomalacia	preterm	20/50–20/40	0.4–0.3
5	male	19	focal cortical atrophy, seizure disorder	Term	20/60–20/60	0.5–0.5
6	male	15	genetic	Term	20/20 - 20/20	0.0–0.0
7	male	16	infection	Term	20/25–20/25	0.1–0.1
8	male	22	periventricular leukomalacia	preterm	20/40–20/25	0.3–0.1
9	male	16	unspecified, developmental delay	Term	20/20–20-20	0.0–0.0
10	male	14	periventricular leukomalacia	preterm	20/25–20/25	0.1–0.1

toys shown in canonical view, presented in a trial by trial fashion, and viewed from an overhead, first-person perspective. Participants were instructed to search, locate, and fixate a specific target toy (a blue truck) placed randomly among surrounding toys (serving as distractors) and without overlap (Fig. 1 A), akin to creating a "pop-out" effect for target detection. A trial consisted of 2 s of viewing of the toy box scene followed by 1 s of a blank gray screen with a central fixation target. This was repeated 25 times per run, with 4 runs collected (total of 100 trials). Each run lasted less than 2 min with a brief rest period between each run. The visual environment was developed using the Unity 3D game engine version 5.6 (Unity Technologies) and on an Alienware Aurora R6 desktop computer (Intel i5 processor, NVidia GTX 1060 graphics card, and 32 GB of RAM; Alienware Corporation). 3D object models were created in house using Blender modeling software (Blender Foundation). The visual task was run using Presentation software (https://www.neurobs.com) to control simultaneous EEG event markers and signal recording (see below).

Participants were seated comfortably 60 cm in front of a 27″ LED monitor (ViewSonic 27" Widescreen 1080p; 1920 × 1080 resolution) (Fig. 1 B). Visual search patterns (X,Y coordinate positions of gaze on the screen) were captured under binocular viewing conditions using a Tobii 4C Eye Tracker system (Tobii Technology AB, Stockholm, Sweden). The system samples gaze data based on pupil center corneal reflections and at a 90 Hz frequency using near infrared illumination. Prior to the first experimental run, eye tracking calibration was performed for each participant (Tobii Eye Tracking Software, v 2.9 calibration protocol) which took less than 1 min to complete. The process included a 7 point calibration task (screen positions: top-left, top-center, top-right, bottom-left, bottom-center, bottom-right, and center-center) followed by a 9 point post calibration verification (the same 7 calibration points plus a center-left and center-right position). Accuracy criterion was determined by gaze fixation falling within a 2.25° (arc degree) radius around each of the 9 points and further confirmed by visual inspection prior to commencing data collection.

2.3. Behavioral data capture, outcome measures, and analysis

As a first level of data analysis, heat maps were generated to characterize visual search area. Captured eye tracking data were aggregated and centered over time to generate heat maps representing the spatial extent of visual search patterns in each participant (Gibaldi et al., 2017).

To further quantify visual search performance, behavioral responses based on eye tracking data were captured as participants initially viewed, searched, located, and then fixated the target. Four objective outcomes were used for this purpose. First, success rate (expressed as a percentage) was determined based on whether a participant was able to find and fixate the target on a given trial. Successful fixation was defined as sustained gaze that remained within the outer contour of the target for a minimum time of 0.4 s. Second, reaction time was defined as the first moment the participant's gaze arrived within the outer contour of the target and fixated the target on the screen for each trial. Third, visual search area was determined based on an ellipse shaped 95% confidence interval fitted to the captured eye tracking data. This was expressed as a percentage of the screen area and represents a measure of visual search precision. Fourth, gaze error was defined as the distance between the center of the target and participant's gaze position. This was computed based on the sampling rate of the eye tracker (90 Hz) and serves as a continuous measure of locating and fixation accuracy of the target (Bennett et al., 2018; Bennett et al., 2021). As a supplemental outcome, we also determined how often/long participants were looking at and away from the screen on a given trial based on the continuous recording of the position of gaze. For this purpose, the off-screen metric represents the number of gaze points per trial that fell outside of the bounds of the screen and thus serves as an index measure of test compliance and reliability (Bennett et al., 2021).

Statistical analyses were carried out using planned independent sample t-tests conducted separately for each of the behavioral measures. All statistical analyses were performed using SAS University Edition statistical package.

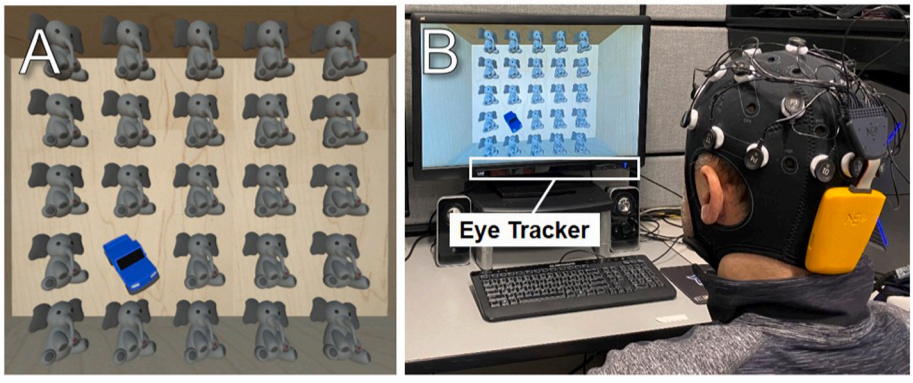

Fig. 1. Experimental Setup. (A) The "virtual toy box" visual search task showing a screenshot of a sample trial. On each trail, the participant was instructed to search for the target (a blue truck) surrounded by distractor toys. (B) Visual search performance was recorded using a screen mounted eye tracker (Tobii 4C Eye Tracker system). EEG recordings associated with task performance were acquired using a wireless montage (Neuroelectrics Enobio 20 channel wireless EEG recording system). (For interpretation of the references to colour in this figure legend, the reader is referred to the Web version of this article.)

2.4. EEG montage, signal processing, and analysis

EEG data were collected using a wireless 20-channel Enobio system (Neuroelectrics, Barcelona, Spain) with a sampling rate of 500 Hz (Fig. 1 B). Electrode placement corresponded to the standard 10–20 international system. After the cap was placed on the participant, conductive gel was added to each electrode site to enhance conductivity between the electrode and scalp surface. The electrodes were made of a solid gel material and each channel fed to a wireless (Bluetooth®) transmitter. An additional reference channel was connected using an ear clip and placed on the participant's right ear lobe. Signals were captured on-line and recorded by software running on a desktop computer located within 1 m of the participant. Once the montage was fully set up, signal quality at each channel was verified and additional conductive gel was added if necessary to ensure adequate signal recording quality.

EEG signal analysis was performed by implementing a validated pipeline (Stropahl et al., 2018; Bottari et al., 2020). Pre-processing of raw EEG data was performed with EEGLAB 13.6.5 b (Delorme and Makeig, 2004). Data were low pass (windowed sinc FIR filter, cut-off frequency 40 Hz, filter order 500) as well as a high pass (windowed sinc FIR filter, cut-off frequency 1 Hz, filter order 100) filtered (Widmann et al., 2015) and then resampled to 250 Hz. To remove non-stereotypical artefacts (e.g., abrupt increases of muscle activity), continuous datasets were segmented into consecutive 1 s epochs. Segments displaying a joint probability of activity (Delorme et al., 2007) exceeding three standard deviations (SD) were removed. To remove typical artefacts associated with eye blinks, an ICA based on the extended Infomax (Bell and Sejnowski, 1995; Jung et al., 2000a, b) was conducted. To reduce computational time, the number of components was set to 15. Resulting ICA weights were then associated to the raw EEG signal (i.e., continuous and unfiltered data). ICA components representing typical artefacts were identified using a data-driven semi--automatic algorithm CORRMAP (Viola et al., 2009). This resulted in the removal of typically 1 or 2 components per participant (controls: mean = 1.08 ± 0.29 SD; CVI: mean = 1.40 ± 0.70 SD). Following the removal of artifact-related components, the data were segmented accordingly to stimuli onsets. The data were segmented into 3 s epochs (comprising −1 to 2 s; full behavioral trial length plus rest). Epochs displaying a joint probability of activity exceeding three standard deviations were automatically rejected. This led to at least 88% of artifact free trials remaining per participant to be used in subsequent time-frequency analysis. Electrophysiological data were subsequently analyzed using the FieldTrip software (Oostenveld et al., 2011).

Epoched data were analyzed performing a time-frequency decomposition. Time–frequency transformation was computed at each channel by convolving the data with a complex Morlet wavelet (t,f0) which had a Gaussian shape in time (σt) and in frequency.

(σf) around the center frequency (f0). Non-constant wavelets increasing from f0/σf = 4 to 13 for frequencies from 3 to 40 Hz (step size 1 Hz) were employed. Time-frequency analyses were conducted per channel using a wavelet transform, known to represent a good balance between time and frequency resolution (Tallon-Baudry and Bertrand, 1999; Bottari et al., 2016). The wavelet transform was conducted for the entire epoch range (−1.000 to 2.000 s) and was done in steps of 0.020 s. The data transformation was performed before averaging across trials, and separately for each frequency band. The total power of each frequency band represented both the phase locked and the non-phase locked signal with respect to the event. The resulting power was baseline corrected to obtain the relative signal change: P(t, f)corrected = (P (t,f)post-stimulus-P(f)baseline)/P(f)baseline. The pre-stimulus period between −700 and −300 msec served as baseline for all spectral analyses. This baseline prevented including eventual slow frequency leakage occurring immediately before the stimulus onset.

The first statistical comparison between groups was done using parametric cluster-based permutation tests (Maris and Oostenveld, 2007). This approach identifies clusters of significant effects in time, frequency, and space and controls for multiple comparisons. Cluster-based permutation analysis was run without a bias from any *a priori* assumptions regarding specific frequency bands, regions of interest (ROI), or time intervals. Thus, it included all channels, frequency range [3–40 Hz], and time-window [0–1 s] after stimulus presentation. A Monte Carlo non-parametric statistical test was used (5000 iterations, cluster alpha = 0.05, maxsum criterion, minimum spatial extent = 1 channel). Identified clusters were considered as being significant at a statistical threshold of $p < 0.025$.

At the group level, baseline-corrected time-frequency representations were computed using a cluster of occipital electrodes (O_1, O_z, and O_2) for each group. 2-D topographical maps of baseline-corrected data were also computed specifically in the peak alpha desynchronization time window (0.5–0.7 s). Furthermore, alpha desynchronization was statistically compared within the post-stimulus peak window (0.5–0.7 s) using paired-sample t-tests for within group comparisons and independent sample t-tests for between group comparisons. Additionally, the same post-stimulus peak window was used for statistical comparisons between alpha desynchronization of each group and 0. Alpha signal in the pre-stimulus window was also statistically compared within an extracted pre-stimulus window (−0.6 to −0.1 s) using an independent sample *t*-test between groups.

2.5. Volume morphometry measures of thalamic nuclei and analysis

Structural morphometry data were available from a subset of participants with CVI (n = 6) who previously participated in an MRI scanning protocol. Two T_1-weighted anatomical scans (TE 3.1 msec, TR 6.8 msec, flip angle 9°, isotropic 1 mm voxel size) were acquired with an 8-channel phased array head coil (Philips 3 T Intera Achieva scanner). The volumes of predetermined thalamic nuclei were quantified for each subject in anatomical space using FreeSurfer (https://surfer.nmr.mgh.harvard.edu) (Dale et al., 1999; Fischl et al., 1999; Fischl et al., 2002; Fischl et al., 2004). Briefly, the two consecutive T_1-weighted volumes were co-registered and averaged to improve signal-to-noise ratio prior to skull stripping, intensity normalization, and Talairach registration. To evaluate specific thalamic nuclei within each participant, 26 thalamic nuclei were isolated in each subject's anatomical space from a probabilistic Morel histological atlas (Niemann et al., 2000; Keller et al., 2012; Iglesias et al., 2018) (see supplementary materials). Residuals were used to remove the effects of intracranial volume on the volume of each segmented thalamic nucleus. These thalamic parcellations show excellent test-retest reliability, good agreeability with stereology, and are robust to abnormal brain morphology (Keller et al., 2012; Iglesias et al., 2018).

A Spearman rank correlation was used to investigate potential associations between alpha desynchronization amplitude and clinical, behavioral, and structural morphometry measures of interest. As this was an exploratory analysis, results were not corrected for multiple comparisons.

3. Results

3.1. Visual search task performance

The CVI group showed an overall impairment in visual search performance compared to controls on all the behavioral outcomes of interest. Qualitatively, we found that controls showed a tight clustering of their visual search area corresponding roughly to the size of the target. Examining data from the CVI group revealed a much larger spatial extent in visual search area compared to controls. Individual heat maps of visual search area for a representative control and participant with CVI are shown in Fig. 2 A and B.

With regard to the four objective outcomes of visual search, we found that the CVI group showed an overall impairment compared to controls (Fig. 2 C - F). Specifically, mean success rate for the CVI group (86.6% ±

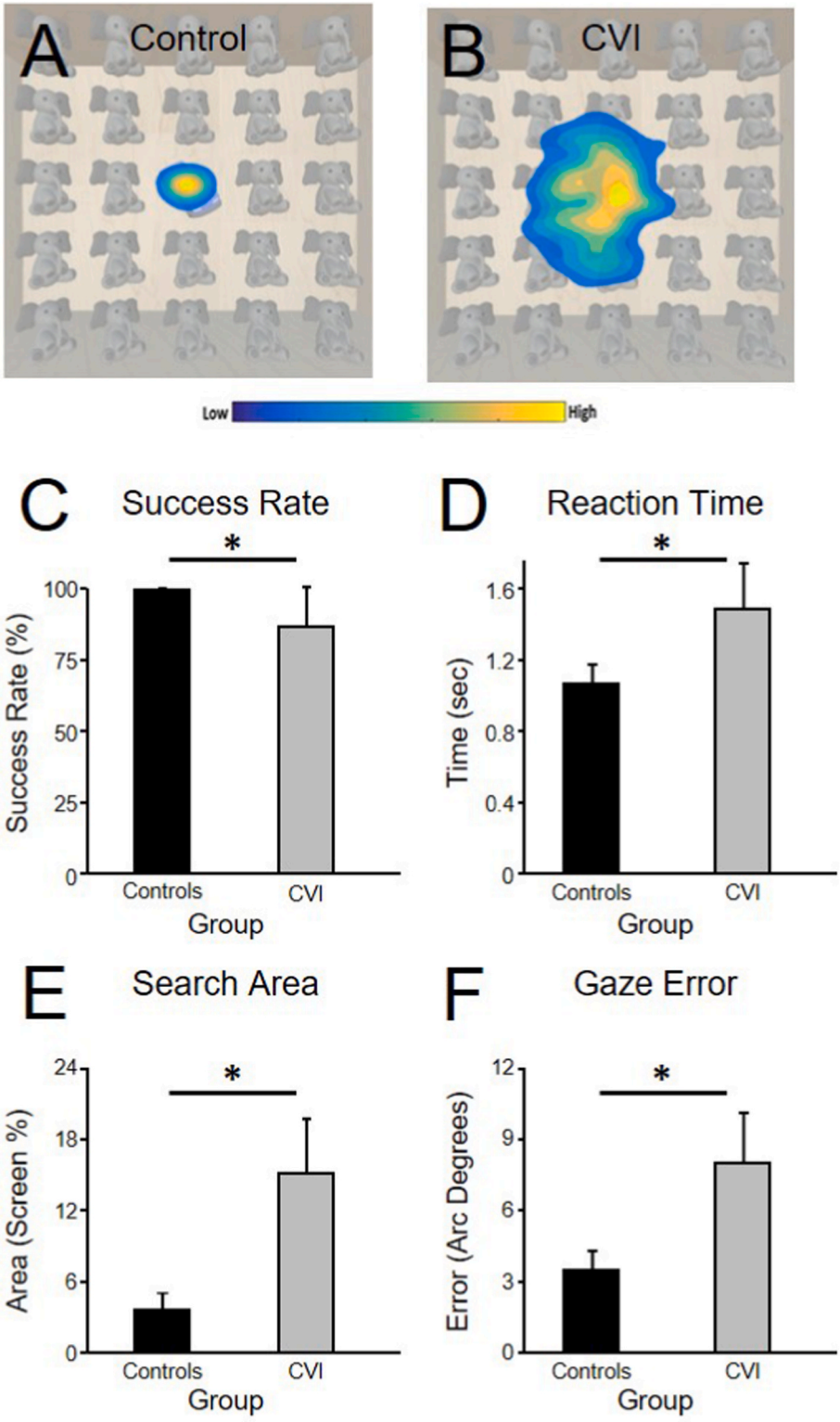

Fig. 2. Visual Search Performance. Heat maps generated from a representative (A) control and (B) CVI participant. Note the larger spatial extent of visual search area in the CVI participant. Group comparisons of (C) success rate, (D) reaction time, (E) visual search area, and (F) gaze error. Individuals with CVI showed an overall impairment in visual search performance compared to controls on all behavioral outcomes of interest (error bars: ± SD; * = $p < 0.05$).

17.71 SD) was lower compared to controls (99.0% ± 2.4 SD). A *t*-test comparison revealed that performance between the two groups was statistically significant [$t(20) = 8.282$, $p < 0.001$]. Mean reaction times for the CVI group (1.467 s ±0.738 SD) were higher than in controls (1.056 s ±0.383 SD) and this difference was also statistically significant [$t(20) = 6.654$, $p < 0.001$]. Mean visual search area was significantly larger for the CVI group (15.044 ± 15.657 SD) compared to controls (3.850 ± 4.582 SD) [$t(20) = 9.745$, $p < 0.001$]. Finally, mean gaze error was significantly higher in the CVI group (8.0875 ± 6.173 SD) compared to controls (3.341 ± 2.843 SD) [$t(20) = 9.709$, $p < 0.001$]. As a supplemental measure, the analysis of mean off-screen data (serving as an index of test compliance and reliability; see Methods) revealed no

statistical difference between the two groups throughout the visual search task (controls = 15.182 ± 12.194 SD and CVI = 16.380 ± 32.513 SD; t = 0.689, p = 0.491).

Examining putative associations between visual acuity (based on the LogMAR value of the better seeing eye) and each of the behavioral visual search outcomes did not reveal any significant statistical correlations (success rate: $r^2 = 0.423$, p = 0.089; reaction time: $r^2 = 0.021$, p = 0.743; visual search area: $r^2 = 0.315$, p = 0.159; gaze error: $r^2 = 0.215$, p = 0.257).

3.2. Analysis of EEG oscillatory activity

Comparisons of the time frequency decomposition analysis of EEG data are shown in Fig. 3. In controls, visual inspection revealed a strong and well-defined alpha desynchronization signal with maximal desynchronization occurring between 0.5 and 0.7 s post stimulus onset (Fig. 3 A, upper panel). In contrast, the response profile in the CVI group appeared to be dramatically altered across low-range frequencies, and in particular, in the alpha range. Specifically, there was a distinct lack of a strong and well defined posterior alpha desynchronization signal (Fig. 3 A, lower panel). Scalp topographies of alpha activity for both groups are displayed in Fig. 3 B (scalp topographies comprise the activity measured within a 60 msec time-window including maximal statistical difference; 0.440–0.500 s).

A cluster-based permutation analysis revealed a significant difference between the CVI group and controls (negative cluster, p = 0.001, see Fig. 4 A and B). This significant effect was largely localized to electrodes within the occipital as well as frontal regions, primarily in the alpha (8–12 Hz) frequency range, and peaked between 0.440 and 0.500 s after stimulus onset. Specific group comparisons in the alpha range revealed a statistically significant difference [t(18) = −4.613, p = 0.002].

A time course plot showing the change in alpha power over time for the occipital channel cluster (O1, O2, Oz) is shown in Fig. 4 C. This plot represents both group means (solid lines) and one standard deviation (shaded areas) for the underlying individual data. There was a separation between the curves for the control and CVI groups that was most evident around 0.3 s post-stimulus onset. This finding is in agreement with previous data, as controls consistently showed a stronger alpha desynchronization signal compared to the CVI group. These group differences were also evident with respect to mean and individual alpha power data (Fig. 4 D; same peak alpha window as used above).

Separate comparisons for each group of alpha oscillations to 0 revealed significant alpha desynchronization for controls [t(11) = −6.238, p = 0.001], but not for the CVI group [t(9) = 1.438, p = 0.194]. This is consistent with a lack of alpha desynchronization signal in the

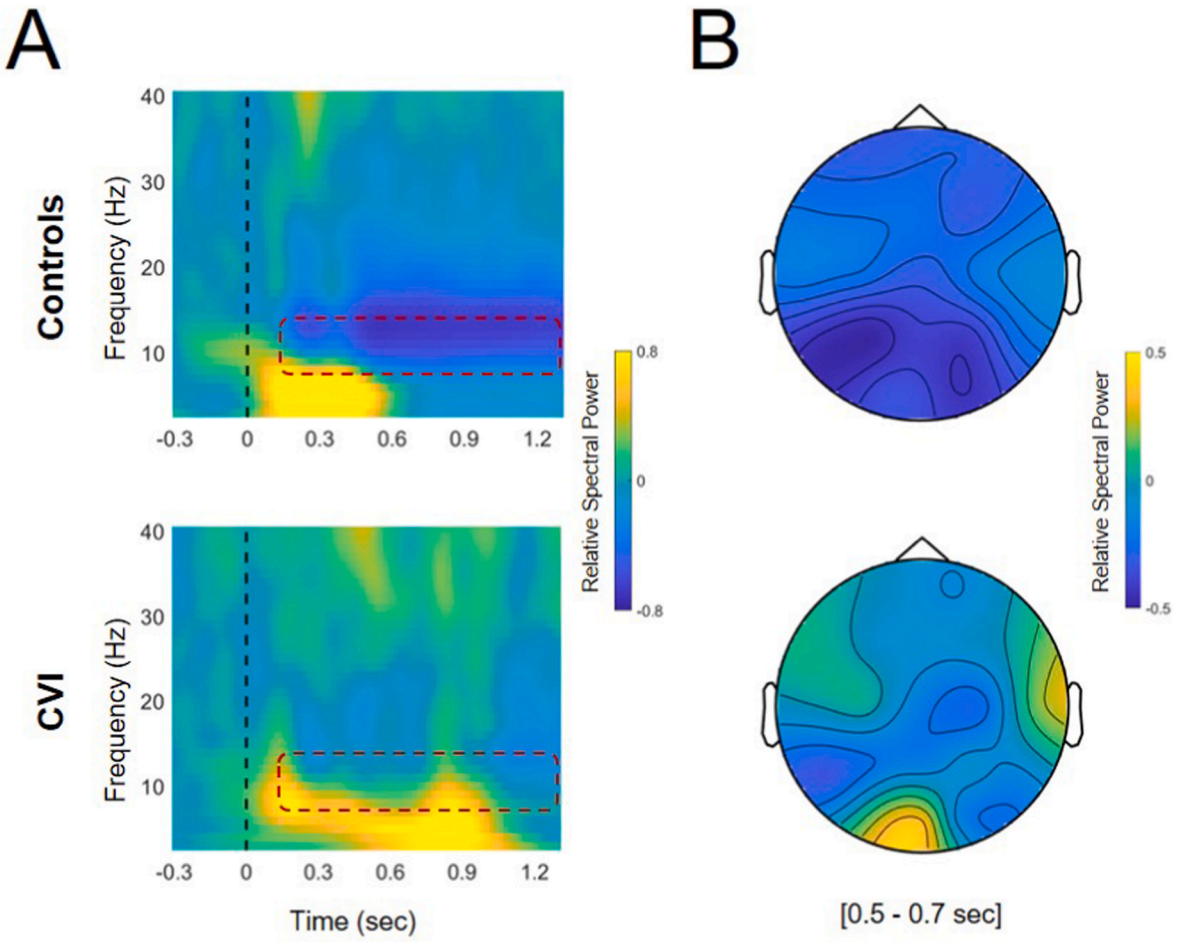

Fig. 3. Time Frequency Plots of Alpha Oscillatory Activity. (A) Relative power signal changes shown in time frequency representations with respect to baseline averaged across the occipital channels (O_1, O_z, and O_2). Data are shown across the frequency range of 3–40 Hz, and for a time window of 0.3 s pre stimulus to 1.2 s post stimulus. Data from each group (CVI and controls) are shown separately. Dotted black line represents stimulus onset. Group differences in alpha desynchronization reveal strong and consistent levels of alpha desynchronization signal in controls that are distinctly absent in the CVI group (see region within dotted line). (B) Scalp topographies of baseline corrected alpha oscillatory activity are shown for the time windows in which group comparisons revealed the highest statistical differences (0.5–0.7 s post-stimulus). Data for each group (controls and CVI) are shown separately. Group differences can be observed at the whole scalp level and in particular, across the posterior electrode locations.

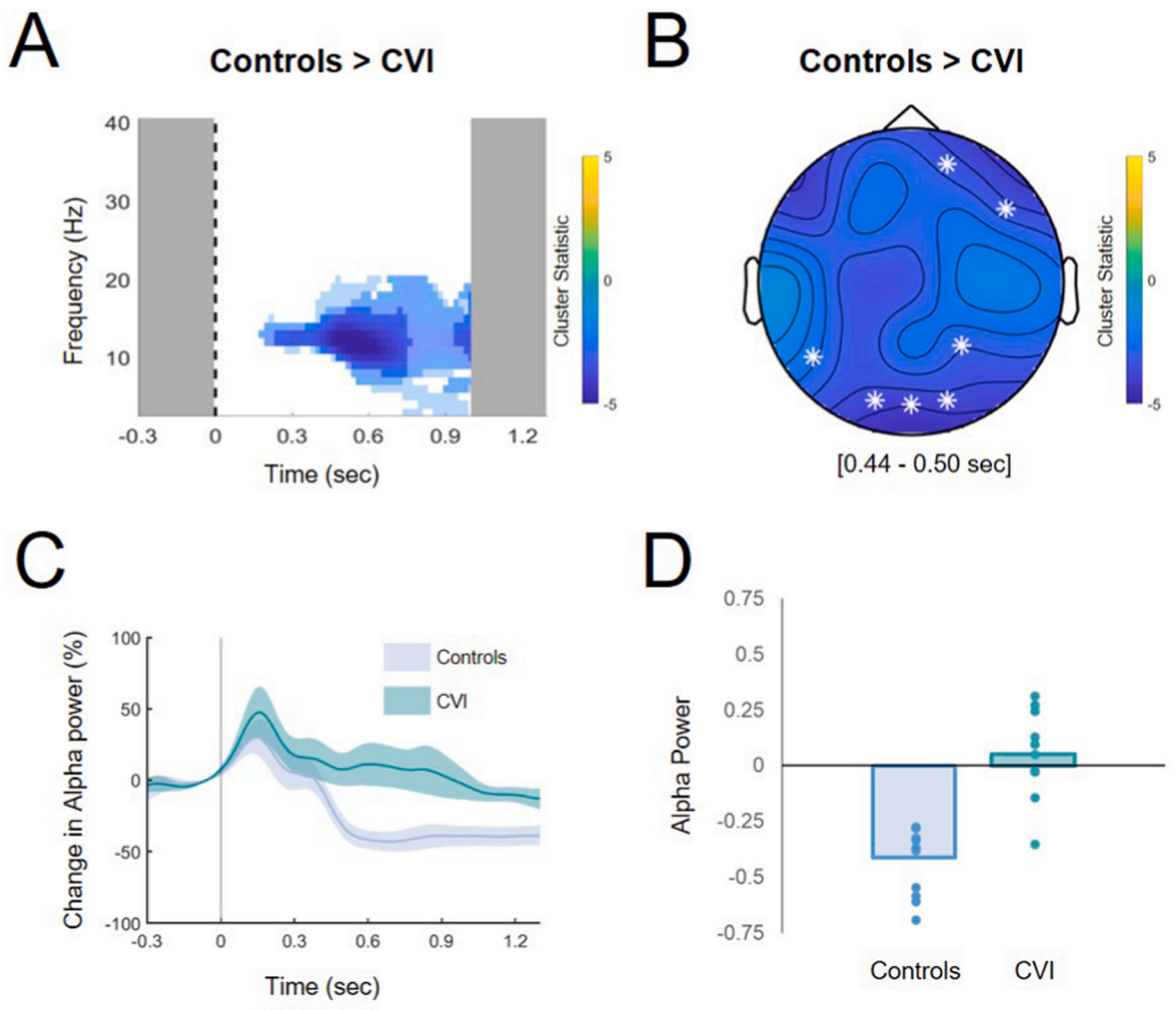

Fig. 4. Alpha Oscillatory Activity and Statistical Comparisons. (A) Cluster-based permutation statistical comparison between groups (Controls > CVI). A statistical comparison was performed within a 0–1 s post-stimulus time window across the frequency range of 3–40 Hz and all electrodes. Significant differences are observed between groups in the alpha range. (B) Scalp topographies of the cluster-based permutation results performed between groups (statistically significant channels highlighted with a white asterisk). (C) Time course plot showing change in alpha power over time for the occipital channel cluster (O1, O2, Oz). Both group means (solid lines) and one standard deviation (shaded areas) are shown. Note the separation between the curves for the control and CVI groups that is most evident around 0.3 s post-stimulus onset. (D) Bar plot showing group differences with respect mean and individual alpha power data.

CVI group during the post-stimulus presentation window.

Finally, an examination was conducted to determine whether alpha oscillatory activity differed between the two groups prior to stimulus onset, and thus potentially influencing post stimulus activity. A statistical analysis was carried out for the time window between −0.6 and −0.1 s prior to stimulus onset. No statistically significant differences (all p's > 0.100) were found between the CVI and control groups with respect to this pre-stimulus window, suggesting that only alpha oscillatory activity occurring after stimulus onset was affected in CVI.

3.3. Correlations between alpha oscillatory activity and behavioral and morphometric measures

Within the CVI group, we conducted an exploratory analysis to investigate putative associations between the amplitude of alpha oscillations and measures of visual function (i.e. visual acuity; n = 10), behavioral performance (n = 10), and structural morphometry at the level of visual thalamic nuclei (n = 6).

Relating alpha desynchronization signal (mean EEG amplitude at 8–12 Hz from time 0.500–0.700 s) and visual acuity (based on the LogMAR value of the better seeing eye) revealed no significant correlation (r^2 = 0.001, p = 0.951). Associating alpha desynchronization signal and behavioral performance revealed a significant correlation with visual search area (r^2 = 0.580, p = 0.037), but not for the other outcome measures (success rate: r^2 = 0.176, p = 0.301; reaction time: r^2 = 0.326, p = 0.151; gaze error (r^2 = 0.510, p = 0.058).

As a last step in the analysis, we explored potential links between alpha desynchronization and the volume of thalamic nuclei. Results from this analysis suggested that there was a significant negative correlation between alpha desynchronization amplitude and the volumes of two thalamic nuclei. Specifically, these were the left ventral lateral anterior (r^2 = 0.69; p = 0.042) and left lateral pulvinar (r^2 = 0.69; p = 0.042) nuclei. In other words, decreased volume of these thalamic nuclei was associated with decreased (i.e. more positive) alpha desynchronization amplitude.

4. Discussion

We present the results of a combined behavioral-EEG paradigm developed for the purposes of characterizing visuospatial processing deficits in individuals with CVI. Specifically, we assessed visual search performance using eye tracking with a novel, behaviorally relevant VR-based task simulating a naturalistic scene (specifically, searching for a toy in a toy box). This was combined with recorded EEG activity, with a

particular focus on analyzing alpha oscillatory responses in relation to visual search performance. We also explored putative associations between magnitude of alpha desynchronization and measures of visual acuity, behavioral performance, and thalamic structural morphometry.

Regarding our behavioral results, we found that individuals with CVI showed an overall impairment in visual search performance as compared to controls. Specifically, we found that the CVI group showed decreased success rate, as well as increased reaction time, visual search area, and gaze error. We interpret these findings to suggest that for our VR-based visual search task, individuals with CVI were more likely to miss and take longer to fixate the target, as well as made less precise and accurate eye movements. These observations are consistent with clinical reports describing deficits with visuospatial processing and attention in this population (Fazzi et al., 2007; Philip and Dutton, 2014; Zihl et al., 2015). It is important to note that this impairment in visual search performance cannot be explained by poor testing compliance in the CVI group. This is supported by the fact that there were no significant differences in terms of captured off-screen data (a measure of task compliance/testing reliability) compared to controls. Furthermore, while success rate was indeed significantly lower in the CVI group compared to controls, the magnitude of effect observed did not appear as large compared to the other behavioral outcomes of interest (i.e. reaction time, visual search area, and gaze error). This indicates that while there was an overall impairment in performance in the CVI group, they were still able to understand and complete the task with a comparatively high level of success. Finally, it is also crucial to highlight that these observed differences in performance cannot be explained by restrictions in visual field, as all participants with CVI had intact visual field function within the area corresponding to the visual stimulus presentation. Moreover, visual search outcomes were not correlated with visual acuity level, and impaired performance was also observed in individuals with normal (or near normal) visual acuity. Taken together, this suggests that observed group differences in our study are likely related to changes in underlying neurophysiology rather than differences related to poor testing compliance and/or measures of visual function.

Analysis of recorded EEG oscillatory activity in response to our visual search task also showed striking differences between the CVI and control groups. In general, the response profile revealed by time-frequency decomposition appeared dramatically altered in the CVI group compared to controls. Specifically, in the CVI group, there was a distinct lack of a strong and well defined posterior alpha desynchronization following stimulus onset compared to controls. We interpret these findings to suggest that in the setting of early neurological damage to retrochiasmatic pathways and visual cerebral structures, the development of alpha desynchronization signals is dramatically altered. Further, there is an impairment in the typical development and deployment of visuospatial and attention systems necessary to carry out our visual search task. We also noted that these differences in alpha desynchronization signals were limited to post-stimulus signal changes, as no significant differences in the pre-stimulus signal were observed between the two groups. This latter finding suggests that differences in alpha desynchronization are largely driven by the modulation of visual system activity following visual stimulus onset, rather than differences in baseline activity or preparatory brain responses. Taken together, our results suggest that the establishment of alpha desynchronization signals associated with visual search performance is dramatically altered in CVI, and may give hints as to the underlying neurophysiological basis regarding visuospatial processing deficits reported in this population.

Finally, we explored putative associations between alpha oscillatory activity and clinical, behavioral, and anatomical measures of interest in the CVI group. Importantly, this analysis revealed that alpha desynchronization signal amplitude was not significantly correlated with visual acuity. That is, the observed neurophysiological alteration was not merely due to an impoverished visual input reaching the visual system. However, analysis of alpha oscillatory activity with respect to behavioral performance and structural morphometry did reveal potential associations of interest. Specifically, we found that the magnitude of alpha desynchronization was significantly correlated with increased visual search area. While this association was not significant with respect to reaction time, visual search area, and gaze error, the overall trend direction was consistent across all visual search outcomes. Furthermore, there was also a significant negative correlation between magnitude of alpha desynchronization and the volumes of the left ventral lateral anterior and left lateral pulvinar nuclei. This is consistent with the notion that decreased volume of these thalamic nuclei is associated with decreased (i.e. more positive) alpha desynchronization. Given that these nuclei are known to be involved with the initiation and control of saccadic eye movements as well as regulation of visual attention (Dominguez-Vargas et al., 2017), we interpret these findings to suggest that impaired visual search performance in CVI is associated with early neurological injury and the maldevelopment of these key visual thalamic nuclei. However, given that morphometric data was available only in a relatively small sample of CVI subjects, these results suggesting a putative association between alpha oscillatory activity and thalamic volume should be interpreted as preliminary.

As mentioned in the introduction, individuals with CVI will often present with impairments related to higher order visuospatial processing and attention (Fazzi et al., 2007; Philip and Dutton, 2014; Zihl et al., 2015), even when measures of visual function (such as visual acuity and visual field) are within normal range (Williams et al., 2011; van Genderen et al., 2012). Thus, the characterization of higher order visual perceptual deficits in CVI remains crucial in order capture a more complete profile of functional visual impairments associated with this condition. Indeed, mounting evidence suggests that impaired visuospatial processing is a common consequence of neurodevelopmental damage (Johnston et al., 2017) and represents the most common type of visual impairment observed in children with CVI (Dutton et al., 2017). Given the profile of higher order visual deficits observed in individuals with this condition, and the role played by the dorsal visual stream in visuospatial processing, CVI has been characterized as a "dorsal stream dysfunction" (Dutton, 2009; Macintyre-Beon et al., 2010); see also "dorsal stream vulnerability" (Braddick et al., 2003)). The results from this study appear to support this view. However, future studies should also investigate behavioral performance (and their neurophysiological correlates) on tasks typically associated with the ventral visual stream in order to further disentangle the nature of observed higher order visual perceptual deficits.

In an attempt to characterize these visuospatial processing impairments in children born premature and with developmental delays, previous studies have used a variety of visual stimuli including biological form from motion, optic flow fields, and spatial integration tasks (e.g. (Braddick et al., 2003; Pavlova et al., 2003; Weinstein et al., 2012)). While these stimulus designs offer control of various testing parameters (e.g. isolating stimulus features), they are not likely to fully capture the subtleties related to higher order visual processing deficits when viewing more complex and naturalistic scenes (similar to the limitations mentioned earlier regarding standard VEP testing). In other words, it is difficult to draw inferences and translate results obtained from these types of psychophysical testing stimuli with respect to how individuals with CVI interact with their visual surroundings. In this direction, our group (as well as others) have incorporated the use of desktop computerized tasks combined with eye tracking metrics to assess ocular motor functions and visual search performance related to higher order visuospatial processing abilities in CVI. For example, using moving cartoon images, Kooiker and colleagues and were able to demonstrate clear deficits related to fixation, ocular motor pursuit, and visual search in children with CVI (Kooiker et al., 2016a, b). In the study presented here, we further expand on the importance of characterizing visual search performance by employing a desktop VR-based task requiring participants to look for a target toy placed within an array of other toys. This novel approach allowed for characterization of functional visual performance using a naturalistic and behaviorally relevant task,

therefore minimizing potential confounds related to poor task comprehension or lack of participant engagement. Furthermore, the inherent design of this VR-based task recruits skills related to real word visual search and attention demands, while affording flexibility to investigate other task related factors such as varying distractor number and characteristics, as well as scene complexity and visual clutter (Bennett et al., 2018).

Previous studies have also attempted to analyze electrophysiological activity beyond that of VEPs tin order to identify the neural correlates associated with visual impairments in CVI. In a recent study, verMass and colleagues (2020) used magnetoencephalography (MEG) to investigate potential differences in oscillatory activity while viewing a high contrast spatial grating stimulus in a cohort of children with cerebral palsy (CP); a neurodevelopmental disorder which often presents in association with CVI. The authors found that in these individuals, viewing visual gratings induced a decrease in alpha-beta (10–20 Hz) activity, and an increase in both low (40–56 Hz) and high (60–72 Hz) gamma oscillations within occipital cortex (VerMaas et al., 2020). Furthermore, the strength of the frequency specifi cortical oscillations were significantly weaker in the children with CP as compared to controls (VerMaas et al., 2020). In another study, neural oscillatory activity within the ventral attention network was recorded while adolescents with CP performed a visual selective attention task (a flanking task where participants were instructed to report the direction of a target arrow while surrounded by congruent or incongruent direction arrows) (Hoffman et al., 2021). Participants with CP were found to have made more errors and had slower responses compared to controls. Interestingly, oscillatory activity recorded by MEG showed that participants with CP had stronger alpha oscillations in the left insula during the incongruent task condition, with stronger responses being associated with worse behavioral performance. The authors interpreted their findings to suggest that aberrant activity within this area was associated with impaired functioning related to visual selective attention (Hoffman et al., 2021). Our results appear to be consistent with these findings of altered neural oscillatory activity linked to impaired visuospatial processing. Specifically, we also observed decreased alpha activity in association with impaired visuospatial processing, and further extend these observations to higher order processing deficits related to visual search performance across multiple etiologies associated with CVI.

The importance of alpha desynchronization signals has been investigated in numerous studies in the context of development, visual deprivation, and acquired posterior brain lesions (such as in the case of hemianopia). Work from human newborn infants (Eisermann et al., 2013), individuals with congenital and profound ocular blindness (Novikova, 1973), as well as following surgical sight restoration (Bottari et al., 2016; Bottari et al., 2018), have provided converging evidence that alpha activity is highly dependent on structured visual experience occurring early in development. For example, EEG recordings from human newborn infants revealed that alpha activity is markedly reduced and shows a developmental time course that normalizes during late childhood (Eisermann et al., 2013). Alpha activity has also been found to be dramatically reduced in adult individuals born with profound ocular blindness (Novikova, 1973). Recent work in humans who underwent sight restoration surgery after a period of congenital blindness (i.e. removal of bilateral dense cataracts) showed that alpha activity is not restored to levels comparable with neurotypical development (Bottari et al., 2016; Bottari et al., 2018). Further evidence supporting the role of posterior occipital cortex in coordinating alpha oscillations is provided from another study recording oscillatory activity in patients with hemianopia due to an acquired posterior brain lesion (Pietrelli et al., 2019). In this study, resting state oscillatory activity was recorded (eyes closed) and a selective slowing of alpha frequency was found in both the intact and the lesioned hemisphere. Furthermore, alpha amplitude was reduced in the lesioned hemisphere resulting in an imbalance in interhemispheric oscillatory activity, with right posterior lesions resulting in a greater reduction in alpha frequency and alteration in interhemispheric balance. Importantly, visuospatial performance (as indexed by impaired visual detection) was associated with alpha frequency duration supporting a functional role of alpha oscillations in visual processing (Pietrelli et al., 2019).

The results of our study expand upon the view regarding the role of alpha oscillatory signals with respect to the integrity and function of the human visual system and brain development. In the case of CVI, we found that the establishment of alpha desynchronization signals occurring during visual processing was dramatically altered despite not having an apparent relationship with standard clinical measures of visual function such as the level of visual acuity and presence of visual field impairment. Thus, even in the case of structured visual experience occurring early in development, damage to central visual processing areas appears to dramatically alter the formation of appropriate visual cortical oscillatory activity, which in turn is associated with higher order visual processing deficits observed in individuals with CVI. This unique opportunity to characterize alpha activity in CVI helps to not only uncover the neurophysiological basis of visual perceptual deficits in these individuals, but also investigate the effect of developmental vulnerability and neuroplasticity in relation to early damage to central visual processing pathways.

While certainly preliminary, our finding of a possible link between the magnitude of alpha desynchronization and the maldevelopment of visual thalamic nuclei in CVI is also of note. Specifically, we found that decreased (i.e. more positive) alpha desynchronization was associated with decreased volume of the left ventral lateral anterior and left lateral pulvinar. This finding may not be surprising given the purported role of these thalamic nuclei in the initiation and control of saccadic eye movements as well as regulation of visual attention (Dominguez-Vargas et al., 2017). Again, these observed associations were the result of an exploratory analysis in a relatively small sample, and further studies with a larger cohort are needed to confirm these preliminary findings. It is also worth highlighting that while the origins of alpha oscillations remain debated, these preliminary findings may also provide cues as to the relative contribution and importance of thalamic integrity with respect to establishing alpha desynchronization activity in humans (Jensen and Mazaheri, 2010). While there is evidence that infragranular layers of the cortex generate alpha rhythm (Da Silva and Van Leeuwen, 1977; Bollimunta et al., 2008; Spaak et al., 2012; Dougherty et al., 2017), several studies have revealed that cortical alpha activity occurs coherently with thalamic activity (Lopes da Silva et al., 1980; Hughes and Crunelli, 2005). Supporting this view, evidence from work in non-human primates suggests that the alpha rhythm generated by the pulvinar is associated with attentional processing occurring at the cortical level (Saalmann et al., 2012).

Finally, a number of limitations with this study need to be considered. First, despite the advantages of associating electrophysiological findings with clinical, functional, and structural morphometry, these conclusions should be interpreted with caution given the relatively small sample size. Despite this issue however, we did observe a very large difference between CVI and control participants with respect to the magnitude of alpha desynchronization (Cohen's d: 1.25; effect size $r = 0.53$). Secondly, identifying participants with CVI who are able to carry out the demands related to a combined behavioral-EEG paradigm (as well as have available morphometric data from MRI structural scans) remains a challenge, and may also lead to a potential selection bias. However, our current study design does present some important advantages. For example, the use of a minimally intrusive wireless EEG recording montage is more amenable for longer periods of signal capture, especially when working with children and adolescents with developmental disabilities. As mentioned previously, the use of desktop VR for the purposes of developing simulations of naturalistic scenes and behaviorally relevant tasks is likely to help better characterize subtle visual processing deficits associated with CVI. Modifications to this visual environment as well as task demands are possible, and will certainly be necessary, in order to accommodate a broader clinical profile.

Finally, while the current study focused on analyzing oscillatory activity within a frequency range related to alpha desynchronization (3–40 Hz), future work will investigate potential differences in other frequency bands. For example, gamma and theta oscillatory activity have been associated with early as well as higher-order visual spatial processing in humans (Kahana et al., 1999; Tallon-Baudry and Bertrand, 1999). Further studies will also consider the analysis of EEG responses in other cortical foci of interest using higher density electrode montages, and with a particular focus on areas associated with the dorsal as well as ventral visual processing streams. This will help further characterize the neurophysiological basis of visual processing deficits in CVI, and their relationship with the timing, severity, type, and location of early neurological damage.

Supplementary Materials. Thalamic Segmentation Map. Location of the 26 segmented thalamic nuclei used in the exploratory correlation analysis. Nuclei were identified based on a probabilistic atlas (Iglesias et al., 2018) and overlaid on axial T1-weighted images from a representative control participant. Note that the data from each hemisphere were evaluated separately. Slice projections move from ventral (left) to more dorsal (right) and are presented in radiologic convention. *Abbreviations:* AV: anteroventral, CeM: central medial, CL: central lateral, CM: centromedian, LD: laterodorsal, LGN: lateral geniculate, LP: lateral posterior, L-Sg: limitans (suprageniculate), MDI: mediodorsal lateral parvocellular, MDm: mediodorsal medial magnocellular, MGN: medial geniculate, MV(Re): reuniens (medial ventral), Pc: paracentral, Pf: parafasicular, Pt: paratenial, PuA: pulvinar anterior, Pul: pulvinar inferior, PuL: pulvinar lateral, PuM: pulvinar medial, R: reticular, VA: ventral anterior, VAmc: ventral anterior magnocellular, VLa: ventral lateral anterior, VLp: ventral lateral posterior, VM: ventromedial, VPL: ventral posterolateral.

Credit author statement

All authors contributed to the design, analysis of results, and preparation of this manuscript. All named authors meet the International Committee of Medical Journal Editors (ICMJE) criteria for authorship for this article. The authors take responsibility for the integrity of the work as a whole, and have given their approval for this version to be published.

Declaration of competing interest

The authors declare no competing interests.

Acknowledgements

This work was supported by grants from the NIH/NEI (R21 EY030587 and R01 EY03097 to LBM and R01 EY030877 to CMB), the Massachusetts Lions Eye Research Fund to CMB and LBM, and the Deborah Munroe Noonan Memorial Research Fund to LBM. The authors also thank Emma Bailin and Timothy Gottlieb for assistance in developing the visual task, as well as the individuals and their families for their willingness to participate in this study.

Appendix A. Supplementary data

Supplementary data to this article can be found online at https://doi.org/10.1016/j.neuropsychologia.2021.108011.

Author contributions

All authors contributed to the design, analysis of results, preparation of this manuscript.

Data availability

The datasets generated during and/or analyzed during the current study are available from the corresponding author upon IRB approval and reasonable request.

References

Aminoff, M.J., 2007. Electrophysiology. Elsevier.
Bell, A.J., Sejnowski, T.J., 1995. An information-maximization approach to blind separation and blind deconvolution. Neural Comput. 7 (6), 1129–1159.
Bennett, C.R., Bailin, E.S., Gottlieb, T.K., Bauer, C.M., Bex, P.J., Merabet, L.B., 2018. Virtual reality based assessment of static object visual search in ocular compared to cerebral visual impairment. HCI 8, 28–38.
Bennett, C.R., Bex, P.J., Bauer, C.M., Merabet, L.B., 2019. The assessment of visual function and functional vision. Semin. Pediatr. Neurol. 31, 30–40.
Bennett, C.R., Bex, P.J., Merabet, L.B., 2021. Assessing visual search performance using a novel dynamic naturalistic scene. J. Vis. 21 (1), 5.
Bollimunta, A., Chen, Y., Schroeder, C.E., Ding, M., 2008. Neuronal mechanisms of cortical alpha oscillations in awake-behaving macaques. J. Neurosci. 28 (40), 9976–9988.
Boot, F.H., Pel, J.J., van der Steen, J., Evenhuis, H.M., 2010. Cerebral Visual Impairment: which perceptive visual dysfunctions can be expected in children with brain damage? A systematic review. Res. Dev. Disabil. 31 (6), 1149–1159.
Bottari, D., Bednaya, E., Dormal, G., Villwock, A., Dzhelyova, M., Grin, K., Pietrini, P., Ricciardi, E., Rossion, B., Röder, B., 2020. EEG frequency-tagging demonstrates increased left hemispheric involvement and crossmodal plasticity for face processing in congenitally deaf signers. Neuroimage 223, 117315.
Bottari, D., Kekunnaya, R., Hense, M., Troje, N.F., Sourav, S., Roder, B., 2018. Motion processing after sight restoration: No competition between visual recovery and auditory compensation. Neuroimage 167, 284–296.
Bottari, D., Troje, N.F., Ley, P., Hense, M., Kekunnaya, R., Röder, B., 2016. Sight restoration after congenital blindness does not reinstate alpha oscillatory activity in humans. Sci. Rep. 6 (1), 1–10.
Braddick, O., Atkinson, J., Wattam-Bell, J., 2003. Normal and anomalous development of visual motion processing: motion coherence and 'dorsal-stream vulnerability. Neuropsychologia 41 (13), 1769–1784.
Capilla, A., Schoffelen, J.M., Paterson, G., Thut, G., Gross, J., 2014. Dissociated alpha-band modulations in the dorsal and ventral visual pathways in visuospatial attention and perception. Cerebr. Cortex 24 (2), 550–561.
Chang, M.Y., Borchert, M.S., 2020. Advances in the evaluation and management of cortical/cerebral visual impairment in children. Surv. Ophthalmol. 65 (6), 708–724.
Clayton, M.S., Yeung, N., Cohen Kadosh, R., 2018. The many characters of visual alpha oscillations. Eur. J. Neurosci. 48 (7), 2498–2508.
Da Silva, F.L., Van Leeuwen, W.S., 1977. The cortical source of the alpha rhythm. Neurosci. Lett. 6 (2–3), 237–241.
Dale, A.M., Fischl, B., Sereno, M.I., 1999. Cortical surface-based analysis: I. Segmentation and surface reconstruction. Neuroimage 9 (2), 179–194.
Delorme, A., Makeig, S., 2004. EEGLAB: an open source toolbox for analysis of single-trial EEG dynamics including independent component analysis. J. Neurosci. Methods 134 (1), 9–21.
Delorme, A., Sejnowski, T., Makeig, S., 2007. Enhanced detection of artifacts in EEG data using higher-order statistics and independent component analysis. Neuroimage 34 (4), 1443–1449.
Dominguez-Vargas, A.U., Schneider, L., Wilke, M., Kagan, I., 2017. Electrical microstimulation of the pulvinar biases saccade choices and reaction times in a time-dependent manner. J. Neurosci. 37 (8), 2234–2257.
Dougherty, K., Cox, M.A., Ninomiya, T., Leopold, D.A., Maier, A., 2017. Ongoing alpha activity in V1 regulates visually driven spiking responses. Cerebr. Cortex 27 (2), 1113–1124.
Dutton, G.N., 2003. Cognitive vision, its disorders and differential diagnosis in adults and children: knowing where and what things are. Eye 17 (3), 289–304.
Dutton, G.N., 2009. Dorsal stream dysfunction' and 'dorsal stream dysfunction plus': a potential classification for perceptual visual impairment in the context of cerebral visual impairment? Dev. Med. Child Neurol. 51 (3), 170–172.
Dutton, G.N., 2013. The spectrum of cerebral visual impairment as a sequel to premature birth: an overview. Doc. Ophthalmol. 127 (1), 69–78.
Dutton, G.N., Chokron, S., Little, S., McDowell, N., 2017. Posterior parietal visual dysfunction: an exploratory review. Vision Development and Rehabilitation 3 (1), 10–22.
Eisermann, M., Kaminska, A., Moutard, M.L., Soufflet, C., Plouin, P., 2013. Normal EEG in childhood: from neonates to adolescents. Neurophysiol. Clin. 43 (1), 35–65.
Fazzi, E., Signorini, S.G., Bova, S.M., La Piana, R., Ondei, P., Bertone, C., Misefari, W., Bianchi, P.E., 2007. Spectrum of visual disorders in children with cerebral visual impairment. J. Child Neurol. 22 (3), 294–301.
Fera, L., Bonito, V., Fiorentini, E., Ubiali, E., 1990. VEP and EEG in cortical blindness: a case with a complicated course. Ital. J. Neurol. Sci. 11 (6), 617–621.
Fischl, B., Salat, D.H., Busa, E., Albert, M., Dieterich, M., Haselgrove, C., Van Der Kouwe, A., Killiany, R., Kennedy, D., Klaveness, S., 2002. Whole brain segmentation: automated labeling of neuroanatomical structures in the human brain. Neuron 33 (3), 341–355.
Fischl, B., Sereno, M.I., Dale, A.M., 1999. Cortical surface-based analysis: II: inflation, flattening, and a surface-based coordinate system. Neuroimage 9 (2), 195–207.

Fischl, B., Van Der Kouwe, A., Destrieux, C., Halgren, E., Ségonne, F., Salat, D.H., Busa, E., Seidman, L.J., Goldstein, J., Kennedy, D., 2004. Automatically parcellating the human cerebral cortex. Cerebr. Cortex 14 (1), 11–22.
Gibaldi, A., Vanegas, M., Bex, P.J., Maiello, G., 2017. Evaluation of the Tobii EyeX eye tracking controller and matlab toolkit for research. Behav. Res. Methods 49 (3), 923–946.
Good, W.V., Jan, J.E., Burden, S.K., Skoczenski, A., Candy, R., 2001. Recent advances in cortical visual impairment. Dev. Med. Child Neurol. 43 (1), 56–60.
Hoffman, R.M., Embury, C.M., Lew, B.J., Heinrichs-Graham, E., Wilson, T.W., Kurz, M.J., 2021. Cortical oscillations that underlie visual selective attention are abnormal in adolescents with cerebral palsy. Sci. Rep. 11 (1), 4661.
Hoyt, C.S., 2003. Visual function in the brain-damaged child. Eye 17 (3), 369–384.
Hughes, S.W., Crunelli, V., 2005. Thalamic mechanisms of EEG alpha rhythms and their pathological implications. Neuroscientist 11 (4), 357–372.
Iglesias, J.E., Insausti, R., Lerma-Usabiaga, G., Bocchetta, M., Van Leemput, K., Greve, D. N., Van der Kouwe, A., Fischl, B., Caballero-Gaudes, C., Paz-Alonso, P.M., 2018. A probabilistic atlas of the human thalamic nuclei combining ex vivo MRI and histology. Neuroimage 183, 314–326.
Jensen, O., Bonnefond, M., VanRullen, R., 2012. An oscillatory mechanism for prioritizing salient unattended stimuli. Trends Cognit. Sci. 16 (4), 200–206.
Jensen, O., Mazaheri, A., 2010. Shaping functional architecture by oscillatory alpha activity: gating by inhibition. Front. Hum. Neurosci. 4, 186.
Johnston, R., Pitchford, N.J., Roach, N.W., Ledgeway, T., 2017. New insights into the role of motion and form vision in neurodevelopmental disorders. Neurosci. Biobehav. Rev. 83, 32–45.
Jung, T.-P., Makeig, S., Westerfield, M., Townsend, J., Courchesne, E., Sejnowski, T.J., 2000a. Removal of eye activity artifacts from visual event-related potentials in normal and clinical subjects. Clin. Neurophysiol. 111 (10), 1745–1758.
Jung, T.P., Makeig, S., Humphries, C., Lee, T.W., Mckeown, M.J., Iragui, V., Sejnowski, T. J., 2000b. Removing electroencephalographic artifacts by blind source separation. Psychophysiology 37 (2), 163–178.
Kahana, M.J., Sekuler, R., Caplan, J.B., Kirschen, M., Madsen, J.R., 1999. Human theta oscillations exhibit task dependence during virtual maze navigation. Nature 399 (6738), 781–784.
Keller, S.S., Gerdes, J.S., Mohammadi, S., Kellinghaus, C., Kugel, H., Deppe, K., Ringelstein, E.B., Evers, S., Schwindt, W., Deppe, M., 2012. Volume estimation of the thalamus using freesurfer and stereology: consistency between methods. Neuroinformatics 10 (4), 341–350.
Klimesch, W., 2012. alpha-band oscillations, attention, and controlled access to stored information. Trends Cognit. Sci. 16 (12), 606–617.
Kooiker, M.J., Pel, J.J., van der Steen-Kant, S.P., van der Steen, J., 2016a. A method to quantify visual information processing in children using eye tracking. JoVE 113.
Kooiker, M.J., Pel, J.J., Verbunt, H.J., de Wit, G.C., van Genderen, M.M., van der Steen, J., 2016b. Quantification of visual function assessment using remote eye tracking in children: validity and applicability. Acta Ophthalmol. 94 (6), 599–608.
Lam, F.C., Lovett, F., Dutton, G.N., 2010. Cerebral visual impairment in children: a longitudinal case study of functional outcomes beyond the visual acuities. J. Vis. Impair. Blind. (JVIB) 104 (10), 625–635.
Lim, M., Soul, J.S., Hansen, R.M., Mayer, D.L., Moskowitz, A., Fulton, A.B., 2005. Development of visual acuity in children with cerebral visual impairment. Arch. Ophthalmol. 123 (9), 1215–1220.
Lopes da Silva, F.H., Vos, J., Mooibroek, J., Rotterdam, A.v., 1980. Relative contributions of intracortical and thalamo-cortical processes in the generation of alpha rhythms, revealed by partial coherence analysis. Electroencephalogr. Clin. Neurophysiol. 50, 449–456.
Macintyre-Beon, C., Ibrahim, H., Hay, I., Cockburn, D., Calvert, J., Dutton, G.N., Bowman, R., 2010. Dorsal stream dysfunction in children: a review and an approach to diagnosis and management. Curr. Pediatr. Rev. 6.
Maris, E., Oostenveld, R., 2007. Nonparametric statistical testing of EEG-and MEG-data. J. Neurosci. Methods 164 (1), 177–190.
Martin, M.B., Santos-Lozano, A., Martin-Hernandez, J., Lopez-Miguel, A., Maldonado, M., Baladron, C., Bauer, C.M., Merabet, L.B., 2016. Cerebral versus ocular visual impairment: the impact on developmental neuroplasticity. Front. Psychol. 7, 1958.
McDowell, N., 2020. A pilot study of the Austin Playing Card Assessment: a tool to detect and find the degree of visual perceptual difficulties related to clutter. Br. J. Vis. Impair. 38 (2), 118–136.
McDowell, N., Dutton, G.N., 2019. Hemianopia and features of balint syndrome following occipital lobe hemorrhage: identification and patient understanding have aided functional improvement years after onset. Case Rep Ophthalmol Med 3864572, 2019.
McKillop, E., Dutton, G.N., 2008. Impairment of vision in children due to damage to the brain: a practical approach. Br. Ir. Orthopt. J. (5), 8–14.
Niemann, K., Mennicken, V., Jeanmonod, D., Morel, A., 2000. The Morel stereotactic atlas of the human thalamus: atlas-to-MR registration of internally consistent canonical model. Neuroimage 12 (6), 601–616.
Novikova, L.A., 1973. Blindness and the Electrical Activity of the Brain: Electroencephalographic Studies of the Effects of Sensory Impairment, vol. 23. American Foundation for the Blind Research Series.
Oostenveld, R., Fries, P., Maris, E., Schoffelen, J.-M., 2011. FieldTrip: open source software for advanced analysis of MEG, EEG, and invasive electrophysiological data. Comput. Intell. Neurosci. 2011.
Parsons, T.D., 2015. Virtual reality for enhanced ecological validity and experimental control in the clinical, affective and social neurosciences. Front. Hum. Neurosci. 9, 660.
Pavlova, M., Staudt, M., Sokolov, A., Birbaumer, N., Krageloh-Mann, I., 2003. Perception and production of biological movement in patients with early periventricular brain lesions. Brain : J. Neurol. 126 (Pt 3), 692–701.
Philip, S.S., Dutton, G.N., 2014. Identifying and characterising cerebral visual impairment in children: a review. Clin. Exp. Optom. 97 (3), 196–208.
Pietrelli, M., Zanon, M., Ladavas, E., Grasso, P.A., Romei, V., Bertini, C., 2019. Posterior brain lesions selectively alter alpha oscillatory activity and predict visual performance in hemianopic patients. Cortex 121, 347–361.
Saalmann, Y.B., Pinsk, M.A., Wang, L., Li, X., Kastner, S., 2012. The pulvinar regulates information transmission between cortical areas based on attention demands. Science 337 (6095), 753–756.
Sakki, H.E.A., Dale, N.J., Sargent, J., Perez-Roche, T., Bowman, R., 2018. Is there consensus in defining childhood cerebral visual impairment? A systematic review of terminology and definitions. Br. J. Ophthalmol. 102 (4), 424–432.
Siegel, M., Donner, T.H., Engel, A.K., 2012. Spectral fingerprints of large-scale neuronal interactions. Nat. Rev. Neurosci. 13 (2), 121–134.
Skoczenski, A.M., Norcia, A.M., 1999. Development of VEP Vernier acuity and grating acuity in human infants. Invest. Ophthalmol. Vis. Sci. 40 (10), 2411–2417.
Solebo, A.L., Teoh, L., Rahi, J., 2017. Epidemiology of blindness in children. Arch. Dis. Child. 102 (9), 853–857.
Spaak, E., Bonnefond, M., Maier, A., Leopold, D.A., Jensen, O., 2012. Layer-specific entrainment of gamma-band neural activity by the alpha rhythm in monkey visual cortex. Curr. Biol. 22 (24), 2313–2318.
Stropahl, M., Bauer, A.-K.R., Debener, S., Bleichner, M.G., 2018. Source-Modeling auditory processes of EEG data using EEGLAB and brainstorm. Front. Neurosci. 12, 309.
Tallon-Baudry, C., Bertrand, O., 1999. Oscillatory gamma activity in humans and its role in object representation. Trends Cognit. Sci. 3 (4), 151–162.
Thut, G., Nietzel, A., Brandt, S.A., Pascual-Leone, A., 2006. Alpha-band electroencephalographic activity over occipital cortex indexes visuospatial attention bias and predicts visual target detection. J. Neurosci. 26 (37), 9494–9502.
Treisman, A.M., Gelade, G., 1980. A feature-integration theory of attention. Cognit. Psychol. 12 (1), 97–136.
van Genderen, M., Dekker, M., Pilon, F., Bals, I., 2012. Diagnosing cerebral visual impairment in children with good visual acuity. Strabismus 20 (2), 78–83.
VerMaas, J.R., Embury, C.M., Hoffman, R.M., Trevarrow, M.P., Wilson, T.W., Kurz, M.J., 2020. Beyond the eye: cortical differences in primary visual processing in children with cerebral palsy. Neuroimage Clin 27, 102318.
Viola, F.C., Thorne, J., Edmonds, B., Schneider, T., Eichele, T., Debener, S., 2009. Semi-automatic identification of independent components representing EEG artifact. Clin. Neurophysiol. 120 (5), 868–877.
Volpe, J.J., 2009. Brain injury in premature infants: a complex amalgam of destructive and developmental disturbances. Lancet Neurol. 8 (1), 110–124.
Watson, T., Orel-Bixler, D., Haegerstrom-Portnoy, G., 2010. Early visual-evoked potential acuity and future behavioral acuity in cortical visual impairment. Optom. Vis. Sci. 87 (2), 80–86.
Weinstein, J.M., Gilmore, R.O., Shaikh, S.M., Kunselman, A.R., Trescher, W.V., Tashima, L.M., Boltz, M.E., McAuliffe, M.B., Cheung, A., Fesi, J.D., 2012. Defective motion processing in children with cerebral visual impairment due to periventricular white matter damage. Dev. Med. Child Neurol. 54 (7), e1–8.
Widmann, A., Schröger, E., Maess, B., 2015. Digital filter design for electrophysiological data–a practical approach. J. Neurosci. Methods 250, 34–46.
Williams, C., Northstone, K., Sabates, R., Feinstein, L., Emond, A., Dutton, G.N., 2011. Visual perceptual difficulties and under-achievement at school in a large community-based sample of children. PloS One 6 (3), 14772.
Zihl, J., Dutton, G.H., 2015. Visual Disorders. Cerebral Visual Impairment in Children: Visuoperceptive and Visuocogntive Disorders. G. N. D. J. Zihl. Springer-Verlag Wien, pp. 61–115.